

## Evaluation of the uncertainty of electrical impedance measurements: the GUM and its Supplement 2

Pedro M Ramos<sup>1</sup>, Fernando M Janeiro<sup>2</sup> and Pedro S Girão<sup>1</sup>

<sup>1</sup>Departamento de Engenharia Electrotécnica e de Computadores, Instituto Superior Técnico, Universidade de Lisboa and Instituto de Telecomunicações, Av. Rovisco Pais, n. 1, 1049-001 Lisbon, Portugal

<sup>2</sup>Instituto de Telecomunicações and Universidade de Évora, Departamento de Física, Rua Romão Ramalho, n. 59, 7000-671 Évora, Portugal

E-mails: pedro.m.ramos@tecnico.ulisboa.pt, fntj@uevora.pt, psgirao@tecnico.ulisboa.pt

**Abstract.** Electrical impedance is not a scalar but a complex quantity. Thus, evaluation of the uncertainty of its value involves a model whose output is a complex. In this paper the comparison of the evaluation of the uncertainty of the measurement of the electrical impedance of a simple electric circuit using the GUM and using a Monte Carlo method according to the Supplement 2 of the GUM is presented.

### 1. Introduction

The publication, in 1993, of the Guide to the Expression of Uncertainty in Measurement (GUM) was the first significant result of the work of more than 15 years developed by individuals and organizations to produce an internationally accepted procedure for expressing measurement uncertainty and for combining individual uncertainty components into a single total uncertainty. The Guide, revised in 1995 and 2008 [1], materializes Recommendation INC-1 (1980) by the CPIM Working Group on the Statement of Uncertainties by providing a conceptual framework allowing a consistent treatment of uncertainty contributions. Complemented by the contribution of many [2-7], the impact of GUM in Metrology was increased when, in 2005, standard ISO/IEC17025 [8] established that accredited test laboratories were required to estimate the uncertainty and to report it. Notwithstanding, the original GUM soon evidenced some shortcomings, namely: (a) dealing with non-symmetrical measurement uncertainty distributions, with non-linearity of the measurement system, with input dependency and systematic bias; (b) it mainly concerns univariate measurement models, namely models having a single scalar output quantity.

To cope with these limitations, work has been developed by many authors (e.g. [9-18]) and two supplements to the GUM – Supplement 1 and Supplement 2 – were issued. Based on the same basic ideas of the GUM – measurement model and probability distribution of the input quantities – Supplement 1 [19], which deals also only with models having a single scalar output quantity, introduces numerical simulation using the Monte Carlo method (MCM) as alternative to analytical or numerical integration for calculating the combination of the probability distributions of the input quantities involved in the propagation of distributions required for the evaluation of measurement



uncertainty. Supplement 2 [20] extends the use of GUM and Supplement 1 to multivariate measurement models, namely models with more than one output quantity. It is true that *the GUM includes examples, from electrical metrology, with three output quantities [JCGM 100:2008 H.2], and thermal metrology, with two output quantities [JCGM 100:2008 H.3]* [20], but Supplement 2 describes a generalization of that Monte Carlo method to obtain a discrete representation of the joint probability distribution for the output quantities of a multivariate model. The discrete representation is then used to provide estimates of the output quantities, and standard uncertainties and covariances associated with those estimates [20].

Supplements 1 and 2 to the GUM originate some inconsistency between the GUM and the Supplements. This fact, added to some non-solved limitations of the GUM itself, lead to the need of a revision of the GUM that, to the best of our knowledge, is underway [21].

The electrical impedance is a simple example of a complex quantity and the output of its measurement model is a complex number. The uncertainty evaluation of electrical impedance measurements using the GUM and using the Supplement 2 to the GUM are compared.

## 2. Electrical impedance

Electrical impedance extends the concept of resistance to alternating current (AC) circuits, describing not only the relative amplitudes of the voltage and current, but also their phase difference. However, electrical impedance measurement is important not only in the analysis of electric circuits but also for other purposes. In fact, because the electrical impedance allows the quantification of the behavior of a conducting medium to an electric current, the impedance measurement is used in the determination of the electromagnetic properties of materials and is the basis of various methods of electrical transduction with applications in fields such as chemistry [22,23] and biomedicine [24-27].

Sometimes abusively used in other time varying regimes, electrical impedance, usually represented by  $Z$ , is an electric quantity defined in the context of sine wave alternating current. Thus if  $v(t)$  is the impedance sinusoidal voltage with constant amplitude  $V_M$ , constant frequency  $f$ , and constant phase  $\varphi_v$

$$v(t) = V_M \cos(2\pi ft + \varphi_v) = \text{Re} \left( V_M e^{j2\pi ft} e^{j\varphi_v} \right), \quad (1)$$

where  $j$  is the imaginary unit and  $\text{Re}(x)$  is the real part of  $x$ , the impedance current is

$$i(t) = I_M \cos(2\pi ft + \varphi_i) = \text{Re} \left( I_M e^{j2\pi ft} e^{j\varphi_i} \right). \quad (2)$$

In complex amplitudes (phasors) both can be written as

$$\bar{V} = V_M e^{j\varphi_v} \quad \text{and} \quad \bar{I} = I_M e^{j\varphi_i}. \quad (3)$$

The impedance is not a phasor but a complex number defined as the ratio  $\bar{V}/\bar{I}$  whose amplitude (module) is  $Z$  and whose phase is  $\varphi$ .

$$\bar{Z} = \frac{\bar{V}}{\bar{I}} = \frac{V_M}{I_M} e^{j(\varphi_v - \varphi_i)} = \frac{V_M}{I_M} e^{j\varphi} = Z e^{j\varphi} = Z \cos(\varphi) + j Z \sin(\varphi). \quad (4)$$

The principles, methods, equipment and procedures for electrical impedance measurement are diverse [28] depending, namely, on the frequency and on the application. In the following sections, and because the purpose here is to compare the uncertainty evaluation using two different methods, the considered case is that of electrical impedance measurements, based on digital acquisition of sinusoidal voltages and estimation of their amplitudes and phase differences as described in [29].

### 3. Results

#### 3.1. Measurement Model

Figure 1 depicts the setup for the measurement of impedance  $Z$  through the measurement of the voltages at its terminals and the terminals of a reference impedance  $Z_R$ . These voltages are buffered with two instrumentation amplifiers (IAs) with unitary gain and simultaneously acquired using two analogue-to-digital converters (ADCs). The series of  $Z$  and  $Z_R$  is excited by the output of a sine wave generator. Figure 2 shows an example of the sampled signals for a 1 kHz measurement frequency. The signal processing algorithm implemented in the DSP estimates the voltage amplitudes and their phase difference using a seven-parameter sine-fitting algorithm [30].

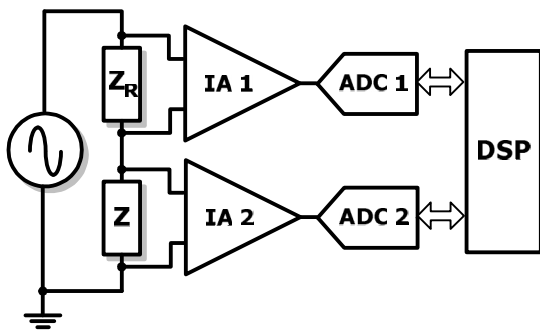


**Figure 1.** Setup for the measurement of  $Z$ .

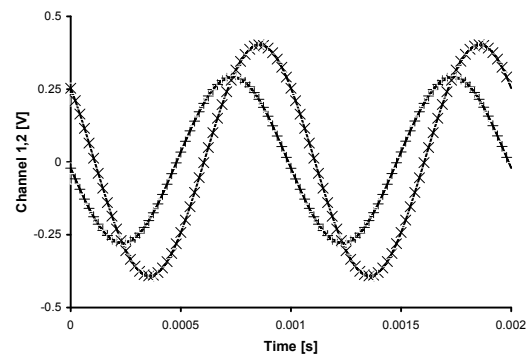


**Figure 2.** Example of ADC 1 and ADC 2 acquired samples.

From Figure 1, and since the input impedance of the IAs is much higher than the amplitudes of both impedances,

$$\frac{\overline{U}_1}{Z_R} = \frac{\overline{U}_2}{Z} \quad (5)$$

where  $\overline{U}_1$  and  $\overline{U}_2$  are the complex amplitudes of the voltage across  $Z_R$  and  $Z$  acquired by ADC 1 and ADC 2, respectively. The impedance measurement model is

$$\overline{Z} = \frac{\overline{U}_2}{\overline{U}_1} \overline{Z}_R. \quad (6)$$

The acquisition process yields an estimation of the complex ratio  $\overline{U}_2/\overline{U}_1$ . The uncertainty of  $Z_R$  (which originates from the measurement of  $Z_R$  with another impedance measurement method) must be included to obtain the uncertainty of  $Z$ .

#### 3.2. Measurements

The results presented correspond to the 1 kHz measurement of an impedance with about 1 k $\Omega$  amplitude and a phase of 5°. The reference impedance also has amplitude near 1 k $\Omega$  and a phase near -85°, which corresponds to a non-ideal capacitor.

In Figure 3, the 2D histogram of the measured  $\overline{U}_2/\overline{U}_1$  ratio is shown for 100 000 measurements with 101 bins both for real and imaginary components. The experimental histogram closely resembles a bivariate normal distribution. Notice that the  $\overline{U}_2/\overline{U}_1$  ratio is located in the complex plane near the

positive imaginary axis. This will result in an impedance near the positive real axis since the reference impedance is a capacitor. The average amplitude ratio value is 0.998619264 while the experimental standard deviation of the mean is  $7.9 \times 10^{-8}$ . The average phase is  $89.5464203^\circ$  with a experimental standard deviation of the mean of  $0.0000034^\circ$ . The coverage regions for 68% and 95% are shown in Figure 4.

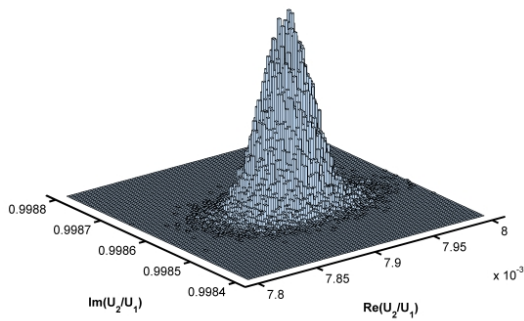


**Figure 3.** 2D histogram of the measured  $\overline{U_2}/\overline{U_1}$  ratio.

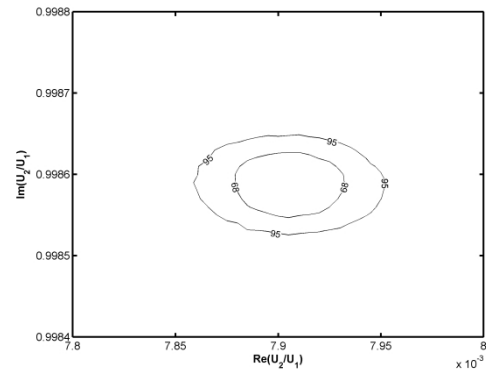


**Figure 4.** Coverage regions for 68% and 95% of the measured  $\overline{U_2}/\overline{U_1}$  ratio.

### 3.3. Uncertainty evaluation following the law of propagation of uncertainty

The use of the law of propagation of uncertainty (LPU) is explained in the GUM [1], but is restricted to measurement models with one scalar output. This method can be applied to the measurement model (6) if it is divided into two: the impedance amplitude and the impedance phase, according to

$$|Z| = \frac{|U_2|}{|U_1|} |Z_R| \quad \text{and} \quad \varphi = \Delta\varphi - \varphi_{Z_R}. \quad (7)$$

In this situation, the combined standard uncertainty of the impedance amplitude is

$$u_{|Z|} = \sqrt{\left(\frac{|U_2|}{|U_1|} u_{|Z_R|}\right)^2 + \left(|Z_R| u_{\frac{|U_2|}{|U_1|}}\right)^2}, \quad (8)$$

since the amplitude ratio measurement and the measurement of the reference impedance are independent. The combined standard uncertainty of the impedance phase is

$$u_\varphi = \sqrt{u_{\Delta\varphi}^2 + u_{\varphi_{Z_R}}^2}. \quad (9)$$

The reference impedance is measured using an AGILENT 4294A. The obtained reference impedance amplitude is  $1004.721 \Omega$  with a maximum error of  $0.76 \Omega$ . As for the phase, the measured value is  $-84.2528^\circ$  with a maximum error of  $0.043^\circ$ . To obtain the uncertainty of the  $Z_R$  measurements (amplitude and phase), the GUM indicates that a uniform probability density function (PDF) should be considered and therefore the uncertainties are obtained by dividing the maximum error by the square root of 3. Notice, that the assumption that the PDF is uniform was validated with consultations with the manufacturer of the impedance meter. Therefore, the standard uncertainty of the reference impedance amplitude and phase are  $u_{|Z|} = 0.44 \Omega$  and  $u_\varphi = 0.025^\circ$ .

In the complex plane, the uncertainty of the impedance amplitude corresponds to an uncertainty in the distance to the origin of the complex number, while the uncertainty of the impedance phase

corresponds to an uncertainty of the complex number phase. The combination of these two uncertainties defines a region with the generic shape depicted in Fig. 8 of [31] and shown in Figure 5. Notice that the considerable distance to origin and the reduced phase uncertainty makes all the lines resemble straight lines when in fact, the real, limits of the coverage phase intervals are arcs.

Another way to interpret the results of the law of propagation of uncertainty is to combine the two outcomes (the amplitude and phase PDFs) considering that they are independent. Since the GUM transforms every uncertainty into a normal PDF distribution, it is possible to combine both output PDFs (amplitude and phase) to obtain a bivariate PDF. The resulting equivalent 2D histogram is shown in Figure 6. Note that, the coverage regions of this histogram (which are ellipses) do not correspond to the intersection areas depicted in Figure 5.

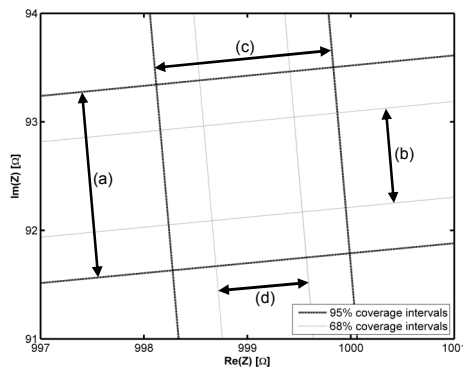


**Figure 5.** Coverage intervals obtained using the LPU. (a) and (b) are the coverage intervals of the impedance phase for 95% and 68%. (c) and (d) are the coverage intervals of the impedance amplitude for 95% and 68%.

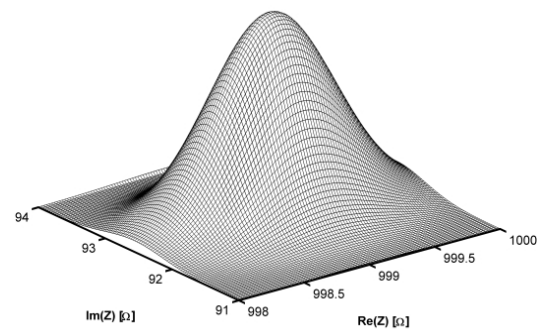


**Figure 6.** Equivalent 2D histogram obtained using the law of propagation of uncertainty as defined in the GUM [1].

### 3.4. Uncertainty evaluation using Monte Carlo method

The law of propagation of uncertainty approach, as shown in the previous section, has significant shortcomings in this (and similar) applications since it neglects any phase/amplitude dependence of the measured  $\overline{U}_2/\overline{U}_1$  ratio and takes a simplistic interpretation of the uncertainty of the reference impedance (transforming the uniform PDFs into normal ones). These shortcomings can be addressed by evaluating the uncertainty of the measurement model (6) using Monte Carlo simulations. In Supplement 1 [19], the use of Monte Carlo method (MCM) is described for single output measurement models where the law of propagation of uncertainty is not suited due to: (a) the type of PDFs of each measurement model input are substantially different from normal PDFs; (b) the first order Taylor approximation used in LPU is not suited for some measurement models; (c) measurement models that cannot be described by a closed algebraic equation (to determine the partial derivatives). Supplement 2 [20], goes further by expanding the use of MCM for measurement models with any number of output quantities. One significant evolution in this supplement is the definition of coverage regions and in particular that of the smallest coverage region (and interval which is also suited for measurement models with a single output).

In the considered case of impedance measurements, the PDF of the reference impedance amplitude is uniform as is the PDF of the reference impedance phase. In order to obtain the histogram of the measured impedance, for each of 100 000  $\overline{U}_2/\overline{U}_1$  ratio measurements, 100 000 values of the reference impedance amplitude and phase are randomly generated in accordance to their uniform distributions. The values of the resulting estimated impedance are then used to generate the 2D histogram (Figure 7) and from the histogram, the coverage region with 95% is obtained (Figure 8).

It can be seen that the 2D histogram is basically a plateau due to the uniform distribution of the reference impedance amplitude and phase. On the edges of the plateau, it decreases quickly (practically following a one-sided normal distribution) due to the relatively narrow 2D histogram of the measured  $\overline{U}_2 / \overline{U}_1$  ratio. Due to the abruptness of the plateau decline, the coverage region for 68% is basically the same as for the 95% case.

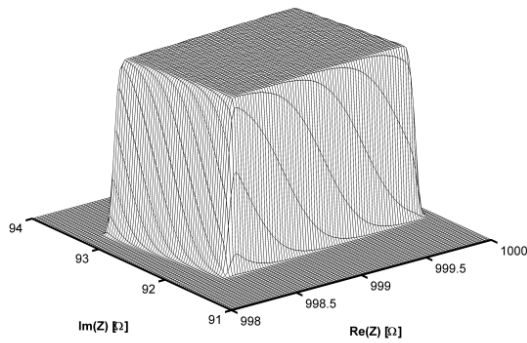


**Figure 7.** 2D histogram of the measured impedance.

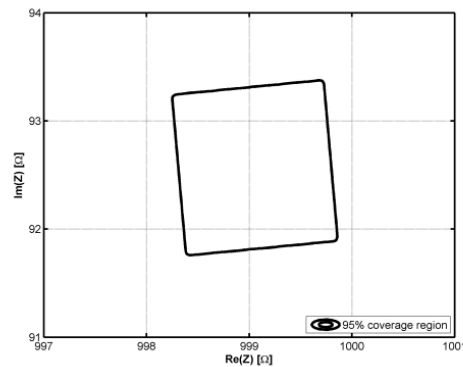


**Figure 8.** Coverage region for 95% of the measured impedance.

One important aspect that should be pointed out, concerns the numerical implementation procedure used to estimate the histogram of Figure 7. The total amount of estimated impedance values is  $10^{10}$ , which would require 160 GBytes of data using a straightforward brute-force approach (herein called the traditional method). This amount of data is unmanageable to process and estimate the final histogram.

The new proposed method consists in processing the data in segments, estimate the 2D histogram contribution of each segment, discard the data and proceed to the next segment storing only the cumulative histogram contribution. In Figure 9, relative simulation times are shown for the new method and that of the traditional method as a function of the number of measured points  $M$  – which is considered to be the same as of the estimated reference impedance values for each measurement – i.e., the total number of estimated impedance values is  $M^2$ . Processing is done in MATLAB on a PC with an i7 processor and 16 GB of RAM.

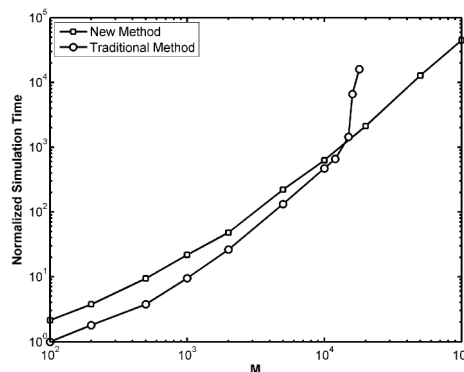


**Figure 9.** Normalized simulation time (ratio between simulation time and the lowest value) to obtain the output histogram as a function of the number of measurements for the traditional method and the new method.

Although the new method is slower for  $M < 10^4$ , due to the multiple histogram assessments, for  $M > 10^4$ , the simulation time of the traditional method increases substantially and for  $M > 18\,000$ , Matlab can no longer conclude the process due to the use of virtual memory and the corresponding increase in access time to the data. On the other hand, the new method has no such constrain and could be used even for  $M > 10^5$ . Note that the amount of required memory for the traditional method is  $16M^2$  Bytes while for the new method it is only  $16M$  Bytes. For  $M = 10^4$ , the traditional method requires 1.6 GBytes, while the new method requires only 160 kBytes.

The drawback of the new method is that the histogram range and its number of points must be defined in the beginning of the process and cannot be changed during the process. This issue requires that the process is started with a low value of  $M$  to define the histogram range, which is refined before the final simulation is executed.

#### 4. Conclusions

The example presented in this paper highlights some of the known limitations of the law of propagation of uncertainty. For this particular case where the estimated output is a complex number, its separation into two measurement models removes the dependency of the estimated complex ratio amplitude and phase. If the real and imaginary components were considered instead, the resulting ellipsoid coverage regions would be different. The Monte Carlo method shows that the actual coverage region is not an ellipsoid but instead a rotated rectangle mainly due to the uncertainty of the reference impedance and its considerable area when compared with the coverage region of the measured complex voltage ratio.

#### 5. References

- [1] BIPM, IEC, IFCC, ILAC, ISO, IUPAC, IUPAP and OIML 2008 Guide to the Expression of Uncertainty in Measurement, JCGM 100:2008, GUM 1995 with minor corrections, <http://www.bipm.org/utis/common/documents/jcgm/JCGM1002008E.pdf>
- [2] Phillips SD, Eberhardt KR, Parry B 1997 Guidelines for Expressing the Uncertainty of Measurement Results Containing Uncorrected Bias *NIST Journal of Research* Institute of Standards and Technology
- [3] Bell S 1999 *A Beginner's Guide to Uncertainty of Measurement* (London: NPL)
- [4] Lira I 2002 *Evaluating the Uncertainty of Measurement. Fundamentals and Practical Guidance* (Bristol, UK: Institute of Physics)
- [5] Kirkup L and Frenkel RB 2006 *An Introduction to Uncertainty in Measurement. Using the GUM (Guide to the Expression of Uncertainty in Measurement)* (Cambridge University Press)
- [6] NASA HDBK-8739.19-3 – Measurement Uncertainty Analysis Principles and Methods, July, 2010
- [7] Willink R, Hall BD 2013 An extension to GUM methodology: degrees-of-freedom calculations for correlated multidimensional estimates”, arXiv:1311.0343 [physics.data-an]
- [8] ISO/IEC 17025:2005 General requirements for the competence of testing and calibration laboratories
- [9] Yeung H and Papadopoulos CE 2000 Natural gas energy flow (quality) uncertainty estimation using Monte Carlo simulation method *International Conference on Flow Measurement, FLOMEKO*
- [10] Khu ST, and Werner MG 2003 Reduction of Monte-Carlo simulation runs for uncertainty estimation in hydrological modelling *Hydrology and Earth System Sciences* **Vol. 7** No. 5 680-690
- [11] Andrae ASG, Miller P, Anderson J and Liu J 2004 Uncertainty estimation by Monte Carlo simulation applied to life cycle inventory of cordless phones and microscale metallization processes *IEEE Transactions on Electronics Packaging Manufacturing* **27** No. 4 233-245

- [12] Rossi GB, Crenna F, Harris PM, Cox MG 2006 Combining direct calculation and the Monte Carlo method for the probabilistic expression of measurement results *Advanced Mathematical and Computational Tools in Metrology VII*, Series on Advances in Mathematics for Applied Sciences vol. 72 221-228, (World Scientific Publishing Co.)
- [13] Cox MG and Bernd Siebert RL 2006 The use of a Monte Carlo method for evaluating uncertainty and expanded uncertainty *Metrologia* **43** 4 178-188
- [14] Silva Ribeiro A 2006, *Avaliação de Incertezas de Medição em Sistemas Complexos Lineares e Não-Lineares*. PhD. thesis (in Portuguese)
- [15] Alves e Sousa J, Silva Ribeiro A, Forbes AB, Harris PM, Carvalho F, Bacelar L 2007 The Relevance of Using a Monte Carlo Method to Evaluate Uncertainty in Mass Calibration *Proc. IMEKO TC3, TC16 & TC22 International Conference* Merida México
- [16] Jing H, Huang M-F, Zhong Y-R, Kuang B and Jiang X-Q 2007 Estimation of the measurement uncertainty based on quasi Monte-Carlo method in optical measurement *Proceedings of the International Society for Optical Engineering*
- [17] Schueller GI 2007 On the treatment of uncertainties in structural mechanics and analysis, *Journal Computers and Structures* **85** 5-6 235-243
- [18] Koch KR 2008 Evaluation of uncertainties in measurements by Monte-Carlo simulations with an application for laser scanning *Journal of Applied Geodesy* **2** 67-77
- [19] BIPM, IEC, IFCC, ILAC, ISO, IUPAC, IUPAP and OIML 2008, Supplement 1 to the 'Guide to the Expression of Uncertainty in Measurement'—Propagation of distributions using a Monte Carlo method JCGM 101:2008, <http://www.bipm.org/utis/common/documents/jcgm/JCGM.101.2008E.pdf>
- [20] BIPM, IEC, IFCC, ILAC, ISO, IUPAC, IUPAP and OIML 2011, Supplement 2 to the 'Guide to the Expression of Uncertainty in Measurement'—Extension to any number of output quantities JCGM 102:2011, <http://www.bipm.org/utis/common/documents/jcgm/JCGM.102.2011.E.pdf>
- [21] Bich W *et al.* 2012 Revision of the 'Guide to the Expression of Uncertainty in Measurement' *Metrologia* **49** 6 702-705
- [22] McNeil CJ, Athey D, Ball M, Ho WO, Krause S, Armstrong RD, Wright JD and Rawson K 1995 Electrochemical Sensors Based on Impedance Measurement of Enzymel Catalyzed Polymer Dissolution: Theory and Applications *Anal. Chem.*, **67**, 3928-3935
- [23] Roy P, Tsai T-C, Liang C-T, Wua R-J and Chavali M 2011 Application of Impedance Measurement Technology in Distinguishing Different Tea Samples with Ppy/SWCNT Composite Sensing Material *Journal of the Chinese Chemical Society* **58** 714-722
- [24] Guimerà A, Calderón E, Los P and Christie AM 2008 Method and device for bio-impedance measurement with hard-tissue applications *Physiological Measurement* **29** 6 15-26
- [25] Tang WH and Tong W 2009 Measuring impedance in congestive heart failure: Current options and clinical applications *Am Heart J.* **157** 3 402-411
- [26] Gupta AK 2011 Respiration Rate Measurement Based on Impedance Pneumography *Texas Instruments Application Report SBAA181*
- [27] Marquez JC, Rempfler M, Seoane F and Lindecrantz K 2013 Textrode-enabled transthoracic electrical bioimpedance measurements – towards wearable applications of impedance cardiography *J Electr Bioimp.* **4** 45-50
- [28] Callegaro L 2013 *Electrical Impedance: Principles, Measurement and Applications* (Boca Raton FL, USA: CRC Press)
- [29] Ramos PM, Silva MF, Serra AC 2004 Low Frequency Impedance Measurement Using Sine-Fitting *Measurement* **35** 89-96
- [30] Ramos PM, Serra AC 2008 A new sine-fitting algorithm for accurate amplitude and phase measurements in two channel acquisition systems *Measurement* **51** 135-143
- [31] Ramos PM, Janeiro FM, Tlemçani M, Serra AC 2009 Recent Developments on Impedance Measurements with DSP-Based Ellipse-Fitting Algorithms *IEEE Transactions on Instrumentation and Measurement* **58** 1680-1689